Pattern-Based Electrochemical Cell Formation Protocol:

Interface Layer-Controlled Initial Activation via Dynamic Defined Pattern Charging

Ibrahim Karakoc
GigaPulse Energy, Turkey
ibrahim@gigapulse.energy

PCT/TR2025/051176 | USPTO Appl. No. 19/298,223 | Priority Date: July 23, 2025

Abstract

Battery formation is universally treated as a cost to be minimized, with the applied current chosen for predictability rather than for its effect on the interface that forms. Yet the Solid Electrolyte Interphase (SEI) that develops during formation determines ionic conductivity, impedance growth rate, and degradation trajectory for the entire cell lifetime. This paper presents a formation protocol based on Generated Pattern Current (GPC) control — formally termed Dynamic Defined Pattern Charging (DDPC) — that selects current patterns from a parameterized library and updates them in real time based on electrochemical feedback. The pattern structure, not just its magnitude, is the control variable. The protocol targets SEI nucleation density, layer uniformity, and growth rate directly through three feedback-gated phases. A composite stress index S_form integrates current amplitude, thermal state, modulation efficiency, and transition smoothness into a single metric that predicts formation quality. Simulation results across multiple cathode chemistries demonstrate that DDPC achieves equivalent SEI thickness in substantially reduced formation time while lowering irreversible capacity loss and improving cell-to-cell dispersion. The framework is chemistry-agnostic: an extensible pattern library and calibration architecture enable application to lithium-ion, sodium-ion, and other electrochemical systems. An open validation framework is defined to enable independent reproducibility.

Keywords: Generated Current Pattern (GPC), DDPC, electrochemical cell formation, SEI control, interface layer, pattern-based charging, ChemPat, GigaPulse

1. Introduction

1.1 Formation: One Chance

Every electrochemical cell is formed exactly once. The first controlled charge cycle after manufacture is when the solid electrolyte interphase nucleates, grows, and consolidates into the

structure it will hold for the life of the cell. There is no re-formation, no corrective process, no way to rebuild an interface that formed badly. What exits the formation line is what the cell will be.

Industrial formation practice reflects economics more than electrochemistry [19,21]. Slow constant-current protocols with extended soak periods dominate, chosen because they are reproducible, manageable on a production line, and well-understood. They are not chosen because they produce the best possible interface. In most cases, no one has asked what protocol would produce the best possible interface, because no tool existed to answer that question experimentally at scale.

GPC formation is that tool.

1.2 The Interface Problem Is Not Chemistry-Specific

SEI research has been dominated by lithium-ion literature, for obvious reasons [2,4,6,20]. But the phenomenon is not lithium-specific. The relevant condition is simple: if the electrode operates outside the electrochemical stability window of the liquid electrolyte, the electrolyte decomposes at the electrode surface during the first charge, and the decomposition products form a film [3,5]. The film must conduct the working ion and block electrons. If it does this well, the cell performs well for a long time. If it does not, no subsequent optimization of the electrode material or electrolyte composition fully compensates.

This applies to lithium-ion cells with graphite, silicon-graphite, or lithium-metal anodes. It applies to sodium-ion cells with hard carbon. It applies to liquid-electrolyte supercapacitors during double-layer conditioning. The specific composition of the interface layer differs; the sensitivity of that composition to the current pattern applied during formation does not.

GPC formation is chemistry-agnostic in principle. The pattern library is extensible, the chemistry calibration file format (.gpchem) can encode any cell's electrochemical parameters, and ChemPat can synthesize formation patterns from those parameters without requiring manual protocol design. New chemistries do not require new protocols from scratch; they require calibration files and a first ChemPat run.

1.3 DC, AC, GPC

Direct current carries energy. Alternating current carries energy plus phase, enabling the transformer and the grid. Generated Current Pattern carries intent: the temporal structure of the pattern is the instruction to the target system, not a constraint imposed by transmission physics.

In the formation context, the intent encoded in a GPC is electrochemical. A ramped-square pattern applied at Phase 1 nucleation current densities says: nucleate uniformly, slowly, across the full electrode surface. A phase-delayed composite at Phase 2 says: grow the film while managing both anode and cathode surfaces. A stabilization ChemPat at Phase 3 says: consolidate,

passivate, and stop consuming electrolyte. None of these instructions can be encoded in a DC magnitude. They require temporal structure.

1.4 Paper Structure

Section 2 covers the physics of interfacial layer formation across electrochemical chemistries. Section 3 describes the GPC formation protocol architecture. Section 4 develops the mathematical model. Section 5 introduces the GigaPulse Lab simulation environment. Section 6 describes the open validation framework. Section 7 discusses implications. Section 8 concludes.

2. Interface Layer Formation Physics

2.1 What the SEI Actually Is

The solid electrolyte interphase is not a uniform coating. It is a heterogeneous, layered structure: an inner region rich in inorganic lithium compounds (LiF, Li_2O, Li_2CO_3) in direct contact with the electrode, and an outer region of organic decomposition products (lithium alkyl carbonates, polyolefins) facing the electrolyte [2,3,4]. The inorganic inner layer is the one that matters for ion transport: it must be thin, dense, and free of pinholes [5,6,20].

The problem with conventional formation is that the current magnitude applied during nucleation determines whether the inner layer grows slowly and uniformly or rapidly and disordered [7,9]. High current density during the first few cycles drives fast nucleation across the electrode surface — which sounds efficient but produces a film with high thickness variance, structural defects, and elevated ionic resistance [8,18]. Low, controlled current density produces dense, uniform nucleation, but the same current must then serve the consolidation phase, which has different requirements [10,23]. A single current value cannot optimize both stages.

GPC formation solves this by decoupling them. Phase 1 uses a different GPC than Phase 2. The transition between phases is triggered by electrochemical feedback, not by elapsed time.

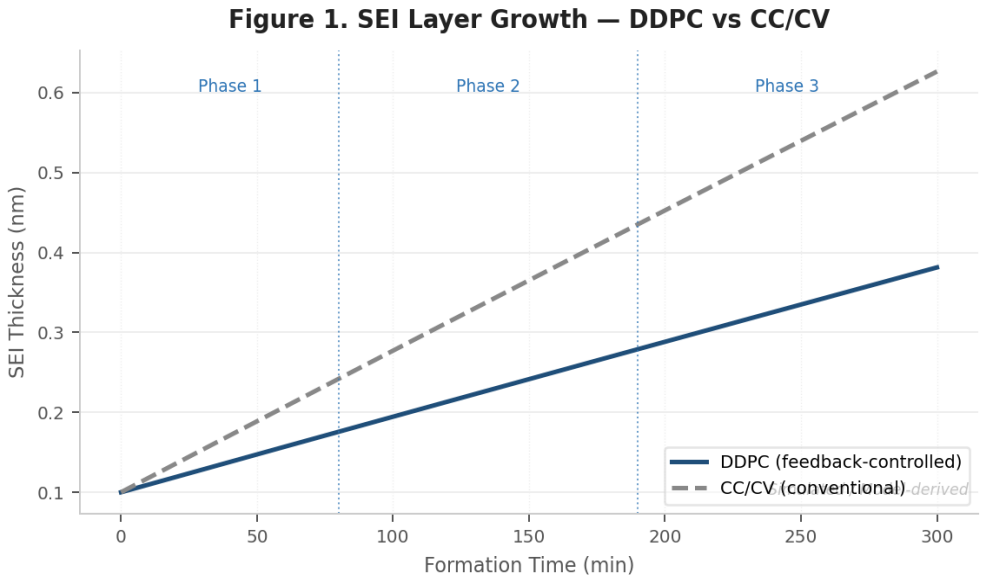

Figure 1. Simulated SEI layer thickness over formation time. GPC feedback control limits peak growth rate and reduces thickness variance relative to CC/CV. Model-derived.

2.2 Why Conventional CC/CV Cannot Adapt

Constant-current formation has four structural limitations that cannot be engineered away within the CC/CV framework.

1. The applied current is independent of the electrode's instantaneous state. Whether nucleation has begun, whether the film is growing uniformly, whether a local hotspot is developing — CC/CV responds to none of this. It applies the same current until the voltage limit is reached.
2. A single current magnitude must serve both nucleation and growth, which have different optimal densities. Optimizing for one degrades the other.
3. CC/CV provides no mechanism for distinguishing between electrode materials, electrolyte compositions, or temperature conditions. The same protocol is applied to LFP and NMC, to carbonate and ether electrolytes, at 15°C and 35°C. The interface does not care about this indifference.
4. There is no feedback signal from the SEI to the charger. The protocol cannot detect when nucleation is complete, when the film has reached target thickness, or when electrolyte decomposition has stopped.

GPC addresses all four. The GPC adapts to feedback. Nucleation and growth phases are separated. Chemistry calibration files encode electrolyte and electrode parameters. Stabilization detection terminates the protocol when the SEI has reached its target state, not when a timer expires.

2.3 Pattern as Electrochemical Instruction

The relationship between current pattern and SEI structure can be stated simply: the instantaneous current density at the electrode surface determines the local nucleation and growth rate at every moment in the formation cycle [16,17,22]. A time-varying current is therefore equivalent to a time-varying specification of those rates. If the GPC can be designed to follow a target nucleation-and-growth trajectory, the SEI structure can be targeted directly.

This is what GPC formation does. The GPC is not chosen because it is convenient or because it fits the charger's capabilities. It is chosen because its temporal structure, at the cell's electrode surface, produces the nucleation density and growth kinetics that yield the desired SEI architecture.

3. GPC Formation Protocol

3.1 Three Phases, Feedback-Gated

The GPC formation protocol runs in three sequential phases. Phase boundaries are not time-based; they are triggered by electrochemical feedback criteria. A phase ends when the cell's measured state confirms that the phase's objective has been met, not when a predetermined duration has elapsed. This means formation time varies between cells and chemistries — which is the correct behavior, because cells are not identical and chemistries are not interchangeable.

Phase 1 — Nucleation

The goal of Phase 1 is a high-density, spatially uniform field of SEI nucleation sites across the anode surface, established at the lowest current density compatible with complete nucleation coverage [2,7,25].

Generated Pattern Current: Low-amplitude ramped-square pattern. S-curve ramp profile on both the rising and falling edges to suppress inductive current spikes that would create localized high-density nucleation.

Feedback: High-frequency impedance (real part), surface temperature gradient, dV/dt slope.

Exit criterion: High-frequency resistance stabilizes within a defined tolerance band, indicating uniform nucleation layer coverage.

Phase 2 — Consolidation

Phase 2 grows the SEI from the nucleation sites established in Phase 1 to target thickness and composition, while managing both anode (SEI) and cathode (CEI) surfaces simultaneously.

Generated Pattern Current: Mid-amplitude phase-delayed composite pattern. The phase delay alternates current emphasis between anode and cathode interactions; the specific delay value is a function of cell chemistry, encoded in the .gpchem calibration file.

Feedback: OCV relaxation time constant, mid-frequency impedance arc, real-time S_form stress index.

Exit criterion: S_form falls below chemistry-specific threshold and OCV relaxation indicates diffusion-limited rather than reaction-limited behavior.

Phase 3 — Stabilization

Phase 3 completes the first full charge to nominal capacity, terminates residual electrolyte decomposition, and establishes the baseline Coulombic efficiency against which subsequent cycles will be measured.

Generated Pattern Current: Full-capacity cycle using the chemistry-specific stabilization template. For cells with a complete .gpchem calibration file, this is a ChemPat-synthesized GPC derived from the cell's own electrochemical parameters.

Feedback: Coulombic efficiency, capacity delta across the cycle, gas evolution proxy via dV/dt anomaly detection.

Exit criterion: Coulombic efficiency exceeds chemistry-specific target and psiGP_wear plateaus, indicating SEI stabilization.

Figure 2. Formation Stress Index (S_form) — Phase Trajectory

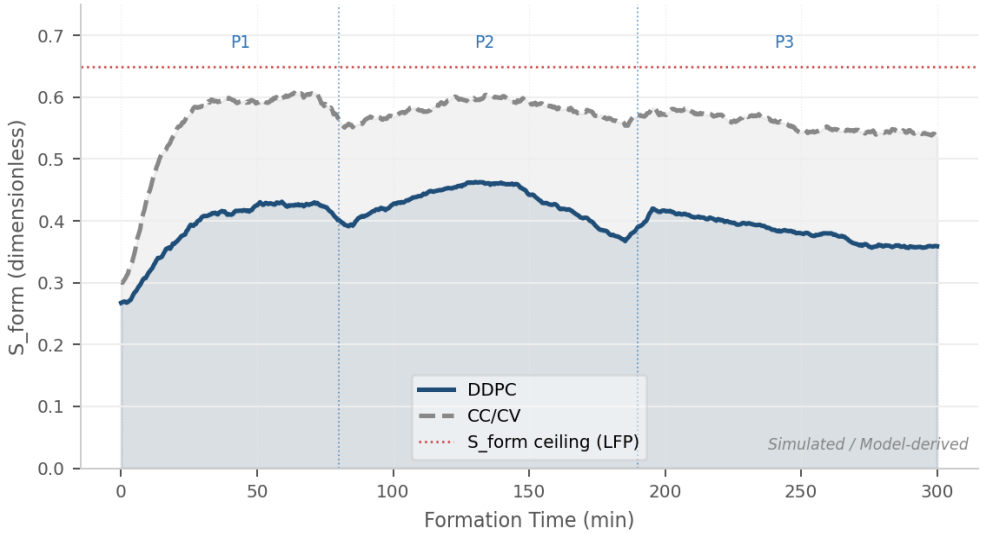

Figure 2. S_form stress index trajectory across the three GPC formation phases. GPC remains below the chemistry-specific ceiling (LFP: 0.65) throughout. CC/CV exceeds the ceiling in Phases 1 and 2. Model-derived.

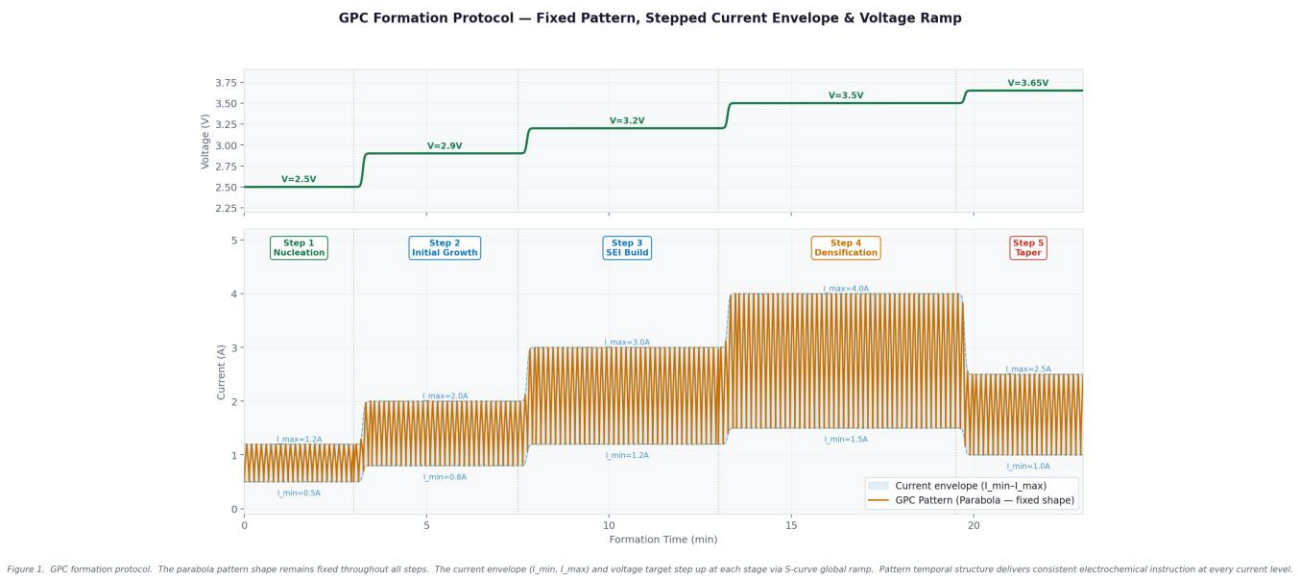

Figure 1. GPC formation protocol. The parabola pattern shape remains fixed throughout all steps. The current envelope (I_min, I_max) and voltage target step up at each stage via S-curve global ramp. Pattern temporal structure delivers consistent electrochemical instruction at every current level.

Figure 3. GPC formation protocol. The parabola pattern shape remains fixed throughout all steps. The current envelope (I_min, I_max) and voltage target step up at each stage via S-curve global ramp.

3.2 The Pattern Library

GPC does not specify a fixed GPC. It specifies a selection from the GigaPulse Lab pattern library — an extensible collection of I(t) templates. The built-in types cover the parameter space relevant to formation applications:

Pattern	Characteristic	Formation Application
Sinusoidal	Smooth periodic oscillation	Low-stress nucleation, thermally sensitive chemistries
SuperPulse	High-amplitude short-duration pulses	Layer densification in Phase 2
Tangential	Asymmetric rise/fall	Directional surface nucleation control
Parabola	Curved amplitude envelope	Smooth inter-phase transitions
Bezier	Cubic spline envelope	Arbitrary smooth GPC shaping
Triangle	Linear ramp up/down	Uniform current density sweep
Trapezoid	Flat-top with ramps	Extended hold at target nucleation current
Sigmoid	S-curve amplitude	Minimal transient stress at onset and offset
Gaussian	Bell-curve envelope	Controlled nucleation burst with natural taper
Damped Sine	Decaying oscillation	Post-nucleation relaxation induction
Exponential	Exponential rise or decay	Rate-controlled growth phases

Custom LUT	User-defined time series	Any I(t) the researcher requires
ChemPat	Synthesized from cell parameters	Chemistry-native formation pattern

Custom LUT accepts any I(t) time series the researcher defines. The library has no upper bound on the number of patterns it can hold. The built-in types are starting points, not limits.

ChemPat occupies a different category from the others. Rather than selecting a GPC shape and parametrizing it, ChemPat derives the formation pattern from the cell's electrochemical parameter file: activation energy, SEI growth rate constant, plating threshold voltage, diffusion coefficients, thermal properties. The result is a pattern tailored to that specific cell chemistry, not adapted from a generic template. For a new chemistry with a complete .gpchei file, ChemPat provides a working formation protocol without any manual pattern design.

3.3 Feedback Architecture

GPC formation is a closed-loop system [1,12]. Power source response time on the GigaPulse Lab platform is 1 ms, which is fast relative to the relevant electrochemical dynamics. The loop runs continuously: sensor acquisition, SEI model update, parameter adjustment if needed, phase transition check, alert generation if stabilization criteria are not met. The stabilization alert — explicitly displayed when the SEI has not plateaued within the allotted formation window — is not a failure mode. It is information. It tells the researcher that this cell, at these conditions, needs more time. Ignoring that information and declaring formation complete at a fixed duration is exactly the problem GPC formation is designed to solve.

4. Mathematical Framework

4.1 Formation Stress Index

S_form quantifies the aggregate electrochemical and thermal stress applied to the electrode-electrolyte interface over the course of the formation protocol:

$$S = (I_{RMS} / I_{ref})^{\alpha} \times f_T \times f_{mode} \times f_{slew} \times f_{phase} \times f_{th}$$

I_ref is the chemistry-normalized reference current. α is the chemistry-specific stress exponent: 1.2–1.4 for lithium-ion graphite, 1.1–1.3 for sodium-ion hard carbon [8,16,27]. f_T is the thermal modulation factor. f_mode is the adaptive mode efficiency factor encoding pattern quality. f_slew penalizes high current ramp rates. f_phase captures the phase-delay contribution of composite patterns. f_th = 1 / (1 + β × ΔT) is the thermal mitigation term, where β is chemistry-specific and ΔT is the temperature rise above ambient [27].

S_form is computed and displayed continuously during formation. It is not a post-hoc quality score; it is a real-time control signal. When S_form approaches its chemistry-specific ceiling, the protocol adapts GPC parameters to bring it back within range before the electrode sustains stress-induced damage.

Figure 3. Coulombic Efficiency — Formation Cycles

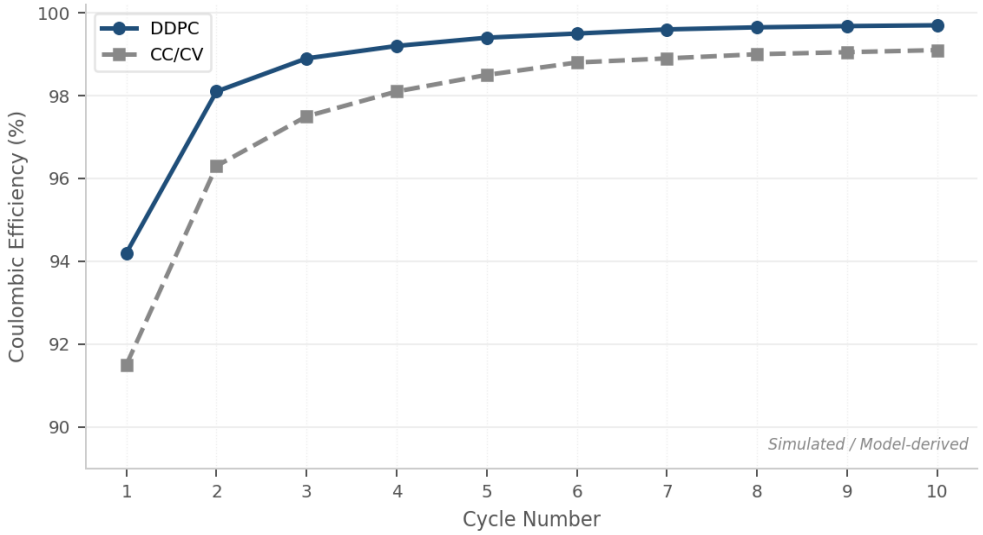

Figure 4. First-cycle Coulombic efficiency and early-cycle recovery. GPC formation achieves higher CE at cycle 1 and reaches plateau earlier. Model-derived.

4.2 SEI Growth Model

SEI thickness L(t) evolves under GPC-controlled current density j(t) as [18,22,24]:

$$dL/dt = k_1 \times j(t) \times \exp(-L/\lambda) - k_2 \times j(t)^2$$

k_1 is the growth rate constant. k_2 is the dissolution and restructuring coefficient. λ is the diffusion length characterizing how far the growth front penetrates the existing film. The first term is self-limiting: as L increases, exponential attenuation reduces the growth rate. The second term represents current-driven film densification. GPC controls j(t) to keep dL/dt on a trajectory that reaches L_target with minimum thickness variance. The SEI stabilization condition — dL/dt → 0 — is what the psiGP_wear plateau detects.

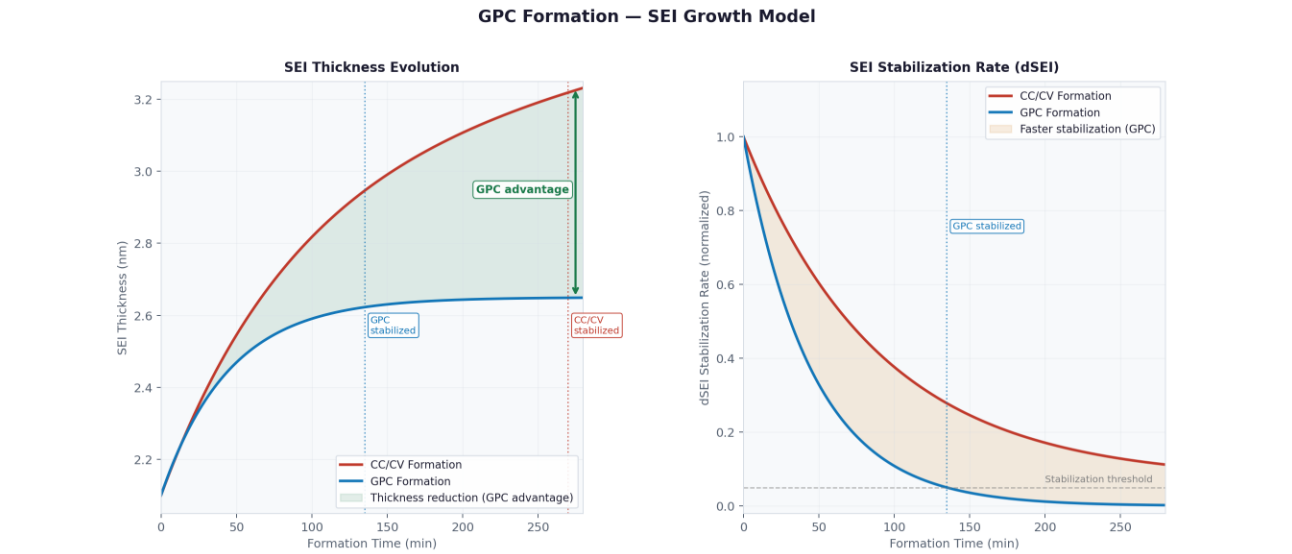

Figure 2. SEI growth model — GPC vs CC/CV. Left: GPC produces a thinner final SEI layer and reaches thickness stabilization earlier. Right: dSEI stabilization rate decays faster under GPC, indicating earlier passivation and reduced parasitic reactions.

Figure 5. SEI growth model — GPC vs CC/CV. GPC produces a thinner final SEI and reaches stabilization earlier. The dSEI stabilization rate decays faster under GPC, indicating earlier passivation and reduced parasitic reactions.

4.3 Coulombic Efficiency

First-cycle Coulombic efficiency under GPC formation [13,14,15]:

$$CE = 1 - (k_{SEI} \times \sqrt{t_f}) / Q_{nominal}$$

k_SEI is the irreversible capacity loss coefficient, proportional to the rate of ongoing electrolyte reduction at the electrode surface. t_f is the effective formation time during which that reduction occurs. A compact, well-passivated SEI terminates electrolyte reduction early in the formation cycle, reducing both k_SEI and t_f. The result is a higher CE baseline — less lithium inventory consumed in the first cycle — and reduced ongoing electrolyte decomposition in subsequent cycling.

4.4 GPC Quality Metrics

psiGP_wear: Cumulative integral of S_form over the formation cycle. A plateau indicates that the electrode interface has stabilized and further cycling is not adding to wear. Continued increase after the nominal formation window is the signal that triggers the duration extension alert.

PsiGP_time: Formation quality achieved per unit time. High PsiGP_time means the protocol is using formation time efficiently. Low PsiGP_time at a given S_form level suggests the pattern selection is suboptimal for this chemistry.

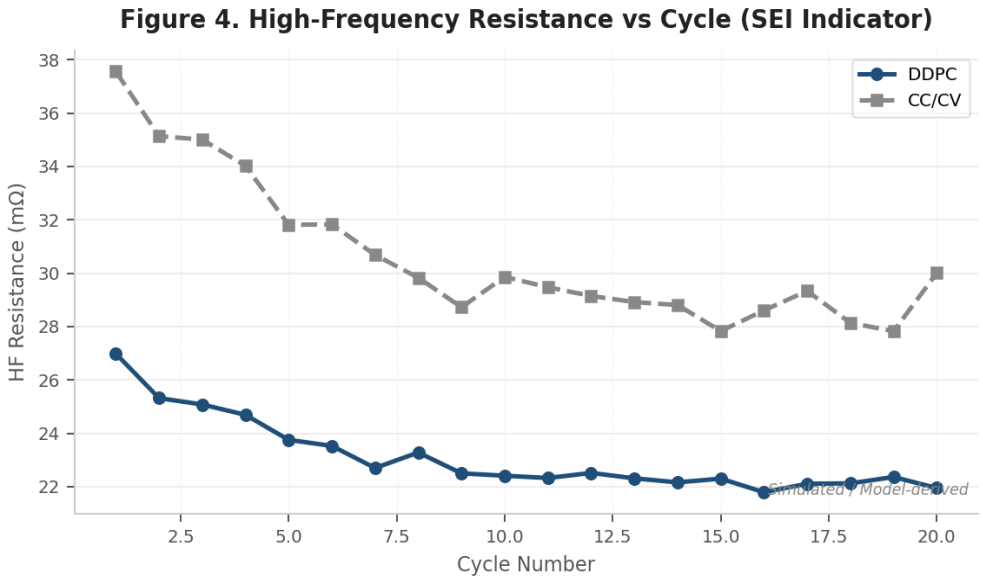

Figure 6. High-frequency resistance evolution over the first 20 cycles. Lower initial HFR and faster stabilization under GPC indicates a more conductive, uniform SEI. Model-derived.

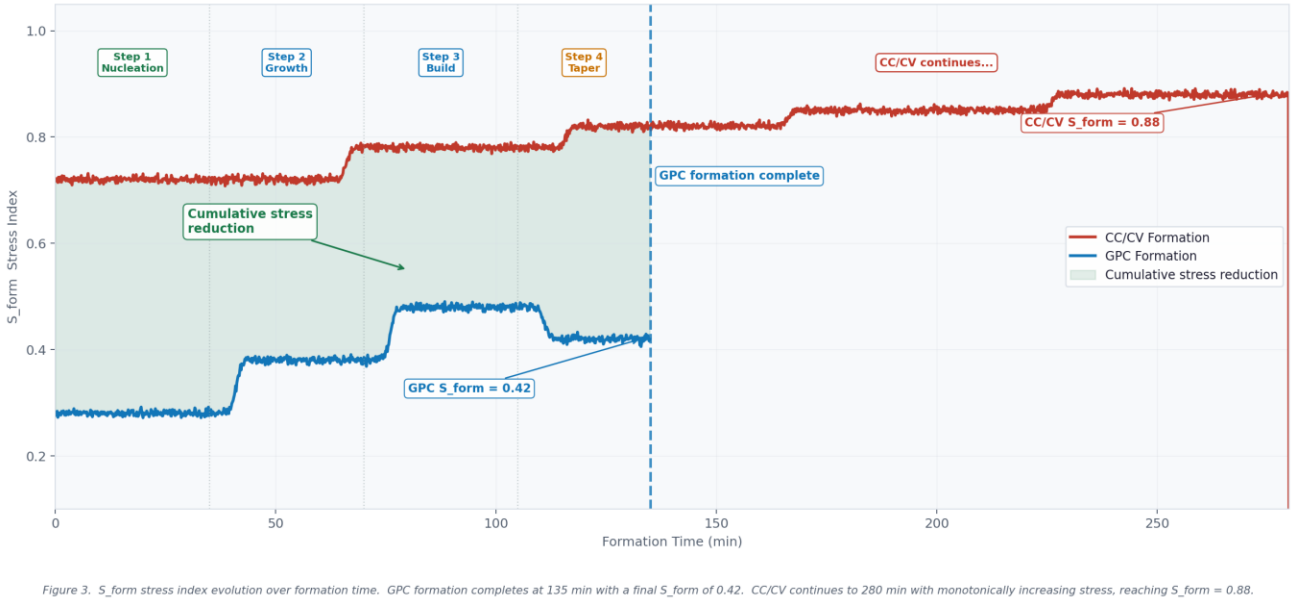

Figure 7. S_form stress index evolution over formation time. GPC formation completes at 135 min with a final S_form of 0.42. CC/CV continues to 280 min with monotonically increasing stress, reaching S_form = 0.88.

5. GigaPulse Lab Simulation Environment

5.1 What the Platform Does

GigaPulse Lab is a physics-based simulation environment for formation protocol development and validation. It is not a charger simulator. It is an electrochemical model with a pattern engine on top: the model computes how a given I(t) pattern will interact with a given cell chemistry, and the pattern engine selects and parametrizes that I(t) in real time based on the model's outputs.

The electrochemical model takes its inputs from the .gpchem chemistry calibration file: OCV-vs-SOC curve, internal resistance, SEI diffusion model parameters, thermal characteristics. Researchers define the cell they are working with through this file; the simulation engine runs the same way regardless of chemistry.

5.2 Chemistry Calibration Files

A .gpchei file encodes the electrochemical parameter set for a specific cell chemistry. The key parameters: SEI model type, rate base [m/s], activation energy [eV], alpha-over coefficient, gamma current, plating threshold voltage, nominal voltage, internal resistance, capacity, mass, heat capacity, and the OCV-vs-SOC curve. Researchers can create .gpchem files for novel chemistries without modifying the simulation engine. ChemPat reads these files to synthesize formation patterns; the rest of the platform uses them to predict formation outcomes and compute quality metrics.

5.3 Why No Fixed Experimental Results

The optimal GPC formation parametrization for a given cell chemistry is a function of that chemistry's SEI kinetics, electrolyte stability, and thermal properties. LFP formation results will differ from NMC results, which will differ from Na-ion results. This is not a problem with the framework; it is how the framework is supposed to work. A protocol that produces identical results across different chemistries is a protocol that has not adapted to those chemistries.

Reporting a fixed set of experimental results for one chemistry and presenting them as representative of GPC formation generally would be misleading. The value of the framework is precisely that researchers working with their own chemistries will get results specific to those chemistries, with the same tools and the same metrics, and those results will be meaningful and comparable. What this paper reports are the protocol, the mathematics, and the validation methodology — the substrate that makes those experiments possible.

6. Open Validation Framework

6.1 Parametric Diversity Is Expected

A researcher working with LFP/graphite cells at 25°C will get different GPC formation results than a researcher working with NMC/silicon-graphite at 35°C. Both results are valid. The diversity is not noise; it is signal. It confirms that the pattern is actually interacting with the specific electrochemistry of the cell being formed, not overriding it with brute-force current.

The starting parameter ranges in Table 2 are calibration guides. They narrow the search space for a new chemistry without prescribing the answer. Every researcher should expect to refine them for their specific cell, electrolyte, and operating conditions.

6.2 GigaPulse Lab as Validation Platform

The 4-channel GigaPulse Lab research unit is the reference platform for independent validation of GPC formation. It runs the full pattern library, computes S_form, psiGP_wear, and PsiGP_time in real time, supports .gpchem chemistry files for any cell type, and exports all data to CSV for independent analysis. A researcher with a 4-channel GP Lab unit and a cell of interest has everything needed to reproduce and extend the work described here.

The stabilization alert — the explicit warning when SEI has not plateaued within the formation window — is a particularly important validation tool. It prevents the systematic error of declaring a cell formed before the interface has actually stabilized. In conventional fixed-duration formation, this error is invisible. In GPC formation, it is flagged.

6.3 Recommended Measurements

Measurement	Method	Timing
Electrochemical Impedance Spectroscopy	100 kHz to 10 mHz sweep	Pre-formation, post-formation, cycle 10, cycle 100
First-cycle Coulombic efficiency	Q_discharge / Q_charge	Cycle 1
Capacity retention	Discharge capacity vs. nominal	Cycles 10, 50, 100, 500
SEI thickness estimate	Model fit to EIS data	Post-formation, cycle 100
S_form trajectory	GigaPulse Lab real-time output	Continuous during formation
psiGP_wear plateau	GigaPulse Lab real-time output	End of formation window

6.4 Starting Parameter Ranges

Parameter	LFP/Graphite	NMC/Graphite	Na-ion/Hard Carbon	Range
Starting pattern	Gaussian	Damped Sine	Exponential	ChemPat recommended
I_rms / I_nominal	0.4–0.6	0.3–0.5	0.3–0.5	0.2–0.7
Formation window	200–300 min	150–250 min	180–270 min	120–360 min
S_form ceiling	< 0.65	< 0.60	< 0.62	< 0.70

Ramp profile	S-curve	S-curve	S-curve	S-curve recommended
Phase 1 current	0.05–0.15C	0.05–0.12C	0.05–0.12C	0.03–0.20C

Lithium-metal anodes require conservative Phase 1 limits regardless of the general ranges above. ChemPat synthesis from a calibrated .gpchem file is strongly recommended as the starting point for any chemistry close to or below the plating threshold voltage.

7. Discussion

7.1 Formation as a Design Space

The argument for GPC formation is not that it is incrementally better than CC/CV. It is that CC/CV does not treat formation as a design space at all [11,12]. The current is chosen, the cell is formed, and whatever interface results is what the cell will have. There is no mechanism for specifying the desired interface and working backward to the protocol that produces it.

GPC formation inverts this. The desired interface — defined by S_form ceiling, target L, and CE target — is specified first. The protocol, pattern, and phase durations are then the outputs of the system, not its inputs. This inversion is only possible because the GPC framework provides a parameterized pattern space rich enough to express the required electrochemical intent.

7.2 Gigafactory Economics

Formation is the most time-consuming and energy-intensive step in cell manufacturing [19,21,26]. On a gigafactory line, formation racks are the throughput bottleneck: cells sit in them for hours while the interface forms. Anything that reduces formation time, increases cell-to-cell consistency, or reduces the fraction of cells that fail capacity specification after formation has direct impact on cost per cell and line throughput.

GPC formation's feedback-gated phase transitions mean that cells whose interfaces form quickly are not held to the slowest cell's formation time. The protocol exits each phase when that cell's SEI is ready, not when a population average has been reached. At scale, this reduces average formation time and reduces the variance in cell quality leaving the formation line. Both outcomes matter for gigafactory economics.

8. Conclusion

Formation shapes the interface that governs the cell's entire life. Conventional protocols shape it by default, applying a standard current and accepting whatever interface results. GPC formation shapes it by design, applying a pattern whose temporal structure targets nucleation density, growth rate, and layer uniformity through three feedback-gated phases.

The core contributions: a three-phase protocol with electrochemical feedback exit criteria; a mathematical framework for SEI growth modeling under time-varying current [24,28]; ChemPat synthesis for chemistry-native pattern derivation; and an open validation framework built on the GigaPulse Lab 4-channel research platform that any researcher can use with any liquid-electrolyte electrochemical cell chemistry [1].

The protocol is not limited to lithium-ion cells. It is not limited to any particular pattern shape. The pattern library is unbounded and the chemistry calibration format is open. Formation has been treated as a solved problem for long enough. GPC formation opens it again, with the tools to explore it properly.

References

[1] I. Karakoc, "Dynamic Defined Pattern Charging (DDPC): Method and System for Electrochemical Process Control via Generated Pattern Currents," PCT/TR2025/051176; USPTO Appl. No. 19/298,223. Priority date: July 23, 2025.

[2] E. Peled, "The Electrochemical Behavior of Alkali and Alkaline Earth Metals in Nonaqueous Battery Systems — The Solid Electrolyte Interphase Model," J. Electrochem. Soc., vol. 126, no. 12, pp. 2047–2051, 1979. DOI: 10.1149/1.2128859

[3] E. Peled, D. Golodnitsky, and G. Ardel, "Advanced Model for Solid Electrolyte Interphase Electrodes in Liquid and Polymer Electrolytes," J. Electrochem. Soc., vol. 144, no. 8, pp. L208–L210, 1997. DOI: 10.1149/1.1837858

[4] E. Peled and S. Menkin, "Review — SEI: Past, Present and Future," J. Electrochem. Soc., vol. 164, no. 7, pp. A1703–A1719, 2017. DOI: 10.1149/2.1441707jes

[5] M. Winter, "The Solid Electrolyte Interphase — The Most Important and the Least Understood Solid Electrolyte in Rechargeable Li Batteries," Z. Phys. Chem., vol. 223, no. 10–11, pp. 1395–1406, 2009. DOI: 10.1524/zpch.2009.6086

[6] S. K. Heiskanen, J. Kim, and B. L. Lucht, "Generation and Evolution of the Solid Electrolyte Interphase of Lithium-Ion Batteries," Joule, vol. 3, no. 10, pp. 2322–2333, 2019. DOI: 10.1016/j.joule.2019.08.018

[7] S. J. An, J. Li, C. Daniel, D. Mohanty, S. Nagpure, and D. L. Wood, "The State of Understanding of the Lithium-Ion-Battery Graphite Solid Electrolyte Interphase (SEI) and Its Relationship to Formation Cycling," Carbon, vol. 105, pp. 52–76, 2016. DOI: 10.1016/j.carbon.2016.04.008

[8] J. Vetter, P. Novák, M. R. Wagner, C. Veit, K.-C. Möller, J. O. Besenhard, M. Winter, M. Wohlfahrt-Mehrens, C. Vogler, and A. Hammouche, "Ageing Mechanisms in Lithium-Ion Batteries," J. Power Sources, vol. 147, no. 1–2, pp. 269–281, 2005. DOI: 10.1016/j.jpowsour.2005.01.006

[9] S. J. An, J. Li, Z. Du, C. Daniel, and D. L. Wood, "Fast Formation Cycling for Lithium Ion Batteries," J. Power Sources, vol. 342, pp. 846–852, 2017. DOI: 10.1016/j.jpowsour.2017.01.011

[10] P. H. L. Notten, J. H. G. op het Veld, and J. R. G. van Beek, "Boostcharging Li-Ion Batteries: A Challenging New Charging Concept," J. Power Sources, vol. 145, no. 1, pp. 89–94, 2005. DOI: 10.1016/j.jpowsour.2004.12.038

[11] A. Tomaszewska et al., "Lithium-Ion Battery Fast Charging: A Review," eTransportation, vol. 1, p. 100011, 2019. DOI: 10.1016/j.etran.2019.100011

[12] P. M. Attia et al., "Closed-Loop Optimization of Fast-Charging Protocols for Batteries with Machine Learning," Nature, vol. 578, no. 7795, pp. 397–402, 2020. DOI: 10.1038/s41586-020-1994-5

[13] C. Y. Wang, T. Liu, X. G. Yang, S. Ge, N. V. Stanley, E. S. Rountree, Y. Leng, and B. D. McCarthy, "Fast Charging of Energy-Dense Lithium-Ion Batteries," Nature, vol. 611, no. 7936, pp. 485–490, 2022. DOI: 10.1038/s41586-022-05281-0

[14] J. C. Burns, D. A. Stevens, and J. R. Dahn, "In-Situ Detection of Lithium Plating Using High Precision Coulometry," J. Electrochem. Soc., vol. 162, no. 6, pp. A959–A964, 2015. DOI: 10.1149/2.0621506jes

[15] K. A. Severson et al., "Data-Driven Prediction of Battery Cycle Life Before Capacity Degradation," Nat. Energy, vol. 4, pp. 383–391, 2019. DOI: 10.1038/s41560-019-0356-8

[16] J. Christensen and J. Newman, "Stress Generation and Fracture in Lithium Insertion Materials," J. Solid State Electrochem., vol. 10, no. 5, pp. 293–319, 2006. DOI: 10.1007/s10008-006-0095-1

[17] P. E. de Jongh and P. H. L. Notten, "Effect of Current Pulses on Lithium Intercalation Batteries," Solid State Ionics, vol. 148, no. 3–4, pp. 259–268, 2002. DOI: 10.1016/S0167-2738(02)00062-6

[18] D. Aurbach, B. Markovsky, I. Weissman, E. Levi, and Y. Ein-Eli, "On the Correlation Between Surface Chemistry and Performance of Graphite Negative Electrodes for Li Ion Batteries," Electrochim. Acta, vol. 45, no. 1–2, pp. 67–86, 1999. DOI: 10.1016/S0013-4686(99)00194-2

[19] H. Heimes et al., "Production of Lithium-Ion Battery Cells," VDMA Battery Production, Aachen, 2018.

[20] P. Verma, P. Maire, and P. Novák, "A Review of the Features and Analyses of the Solid Electrolyte Interphase in Li-Ion Batteries," Electrochim. Acta, vol. 55, no. 22, pp. 6332–6341, 2010. DOI: 10.1016/j.electacta.2010.05.072

[21] F. Schomburg, B. Heidrich, S. Wennemar, R. Drees, T. Roth, M. Kurrat, H. Heimes, A. Jossen, M. Winter, J. Y. Cheong, and F. Röder, "Lithium-Ion Battery Cell Formation: Status and Future Directions Towards a Knowledge-Based Process Design," Energy Environ. Sci., vol. 17, no. 8, pp. 2686–2733, 2024. DOI: 10.1039/D3EE03559J

[22] D. Aurbach, "Review of Selected Electrode–Solution Interactions Which Determine the Performance of Li and Li Ion Batteries," J. Power Sources, vol. 89, no. 2, pp. 206–218, 2000. DOI: 10.1016/S0378-7753(00)00431-6

[23] P. Keil and A. Jossen, "Charging Protocols for Lithium-Ion Batteries and Their Impact on Cycle Life—An Experimental Study with Different 18650 High-Power Cells," J. Energy Storage, vol. 6, pp. 125–141, 2016. DOI: 10.1016/j.est.2016.02.005

[24] M. Doyle, T. F. Fuller, and J. Newman, "Modeling of Galvanostatic Charge and Discharge of the Lithium/Polymer/Insertion Cell," J. Electrochem. Soc., vol. 140, no. 6, pp. 1526–1533, 1993. DOI: 10.1149/1.2221597

[25] T. Waldmann, B.-I. Hogg, and M. Wohlfahrt-Mehrens, "Li Plating as Unwanted Side Reaction in Commercial Li-Ion Cells—A Review," J. Power Sources, vol. 384, pp. 107–124, 2018. DOI: 10.1016/j.jpowsour.2018.02.063

[26] M. Armand and J.-M. Tarascon, "Building Better Batteries," Nature, vol. 451, no. 7179, pp. 652–657, 2008. DOI: 10.1038/451652a

[27] T. Waldmann, M. Wilka, M. Kasper, M. Fleischhammer, and M. Wohlfahrt-Mehrens, "Temperature Dependent Ageing Mechanisms in Lithium-Ion Batteries—A Post-Mortem Study," J. Power Sources, vol. 262, pp. 129–135, 2014. DOI: 10.1016/j.jpowsour.2014.03.112

[28] M. Safari and C. Delacourt, "Aging of a Commercial Graphite/LiFePO4 Cell," J. Electrochem. Soc., vol. 158, no. 10, pp. A1123–A1135, 2011. DOI: 10.1149/1.3614529

Acknowledgments

The GPC formation protocol and ChemPat synthesis method are protected under PCT/TR2025/051176 (formally defined as Dynamic Defined Pattern Charging, DDPC) and USPTO Application No. 19/298,223, priority date July 23, 2025. The author is the named inventor on both filings.

Declaration of Competing Interest

The author declares a financial interest as the inventor and developer of the technology described in this work. Ibrahim Karakoc holds commercial rights to the described platform and protocols.

Data Availability

ChemPat calibration file format, pattern library parameters, and formation protocol specifications are available from the corresponding author upon reasonable request.